Experimental Analysis of the Utility of Liquid Metal Gallium as a Contrast Agent for CT Hepatic Artery Angiography in Living Rabbits

Ting Liu
the Third Medical Centre of Chinese PLA General Hospital,The Training Site for Postgraduate of Jinzhou Medical University

Sheng Wang
the third Medical Centre of Chinese PLA General Hospital

Wei Zhao
the Third Medical Centre of Chinese PLA General Hospital,The Training Site for Postgraduate of Jinzhou Medical University

Hao Liu
the third Medical Centre of Chinese PLA General Hospital

Yi Zhang
the third Medical Centre of Chinese PLA General Hospital

Juan Han
the third Medical Centre of Chinese PLA General Hospital

Xia Chen (xiaoxia0905@126.com)
the third Medical Centre of Chinese PLA General Hospital

Research Article

Keywords: CT angiography (CTA) technology, adverse drug reactions (ADRs), allergies , drug toxicity

Posted Date: December 30th, 2020

DOI: https://doi.org/10.21203/rs.3.rs-135998/v1

Abstract

CT angiography (CTA) technology, as a non-invasive or minimally invasive examination method, is commonly used in the clinic to obtain vascular network images, and iodinated contrast agents play a vital role in it. At present, the second-generation non-ionic contrast agent ioversol are most commonly used in CTA, but its preparation process is complicated, the manufacture technology of it is high, and it is associated with some adverse drug reactions (ADRs), such as allergies and drug toxicity. In this work, based on the low melting point (29.78℃) and low viscosity of liquid metal gallium, it was used for the first time as an angiographic contrast agent for in vivo hepatic artery angiography. According to the statistical analysis of the smallest visible diameter of the hepatic artery and the contrast effect between the blood vessels and their surrounding tissues in CT images, we confirmed that compared with CT imaging using ioversol for hepatic artery angiography, that using liquid metal gallium produced more intuitive and excellent vascular imaging effects.In other words, the use of liquid metal gallium as an angiographic contrast agent has a certain value in living organ angiography. However, the lower overall image quality and higher side-effects of liquid metal gallium in CTA indicate that the use of liquid metal gallium as a contrast agent for living organs still needs to overcome some problems, such as the metallic artefacts and its hypertonicity. Only in this way can liquid metal gallium become a potential contrast agent candidate for angiography in animal experiments and possibly even in the clinical.

Background

In the inspection and diagnosis of benign and malignant tumours, cardiovascular diseases, vascular dysplasia, aortic dissections and other diseases, the distribution of blood vessels is an important index to evaluate the occurrence and progression of the disease [1]. Therefore, obtaining high-quality vascular network imaging is of great significance for tissue physiology, pathology, anatomy and imaging diagnostics. Hounsfield first developed computed tomography (CT) in 1973, and CT has developed rapidly in the last half-century [2]. For example, 320-slice CT can complete a circle scan in only 0.35 seconds [3], so that the entire organ can be imaged in an instant, and after multiple circle scans, the activity and blood flow of the whole organ can be displayed in real-time. The three-dimensional dynamics are very vivid, providing a non-invasive or micro-invasive CT angiography (CTA) examinations that have increasingly become an important and common vascular inspection method in the clinic [4]. CT angiography vividly shows a large density difference on CT imaging by comparing the contrast agent concentration difference formed by different concentrations of contrast agent in blood vessels or different blood supplies to tissues, to increase the contrast between blood vessels and tissues, and provide abundant and accurate information for clinical diagnosis and treatment. In this process, iodinated contrast agent plays a vital role [5].

Nonionic iodine contrast agent is a triiodobenzene compound (Fig. 1) that is obtained by replacing the carboxyl group on the benzene ring of the ionic contrast agent with an amide group [6]. This change in chemical structure prevents ionization in the solution and the toxicity of its penetration is significantly

lower than that of ionic iodine contrast agents. In addition, the six hydroxyl groups evenly distributed around the benzene ring of the non-ionic iodine contrast agent effectively shield the fat-soluble iodophenyl group, so that non-ionic iodine contrast agent has gradually replaced ionic contrast media in most clinical applications [7]. However, it has the disadvantages of a complicated preparation process, high technical requirements, and a high price, and it can trigger adverse drug reactions (ADR) [8,9]. Among them, allergic reactions to iodinated contrast agents are a major risk during CTA examinations[10,11]. The clinical manifestations of mild anaphylaxis include nausea, vomiting, diarrhoea, conjunctiva congestion, cold sweats, coughing, sneezing, facial paleness, etc. Karoline et al. found in a phase II clinical trial of iomethol that some patients had severe itching of their head and face, repeated urticaria and other allergic reactions [12]. Moderate allergic reactions can cause urticaria-like erythema with itching; oedema of the eyelids, cheeks, lips, and face; chest congestion; hoarseness and trembling limbs. Severe allergic reactions include a pale complexion, bruising of the limbs, cold hands and feet, difficulty breathing, muscle spasms, decreased blood pressure, loss of consciousness, incontinence, and even anaphylactic shock or cardiac arrest [13,14,15].

In addition, contrast-induced nephropathy (CIN), the most common adverse reaction in the urinary system caused by non-ionic iodized contrast agents, has become the third leading cause of acute kidney injury among inpatients, second only to renal hypoperfusion and drug-induced acute kidney injury, accounting for approximately 11% of the total acute kidney injury in hospitalized patients [16,17,18,19]. In a coronary angiography study involving 319 patients, Burch ADRt et al. found that most patients had serum creatinine (SCr) levels and blood urea nitrogen (BUN) increases within 12 to 18 hours after the injection of the contrast agent, and their glomerular filtration and creatinine clearance rate (CCR) were decreased [20].

Gallium is in the IIIA group of the periodic table and is a semi-metallic element. It has a melting point of 29.78°C, a density of 5.804 g/cm^3 in a solid state, a density of 6.095 g/cm^3 in a liquid state, and a viscosity of 1.2 (77°C) mPa/s. It forms a stable liquid at body temperature, and its production process is simple, its cost is relatively low, its chemical properties are relatively stable, and its activity is weaker than that of aluminium. As an environmentally friendly material, it is much safer than liquid metal mercury[21,22,23].

The earliest use of gallium in medicine was in the diagnosis of tumours. 67 Ga has its highest absorption rate in nonosseous tumours in animals [24], and it can exist in living tumour cells [25]. In addition, gallium compounds have antitumour activity against lymphoma, advanced malignant melanoma, ovarian carcinoma, and soft tissue sarcoma, among which gallium nitrate has the strongest anticancer activity [26,27,28,29,30,31]. It has also been demonstrated that some gallium compounds, such as gallium nitrate III, has antibacterial effects against *Francisella tulerens* [32], *Klebsiella pneumoniae* [33], and *Pseudomonas aeruginosa* [34]. Moreover, liquid metal gallium can also be used as an antiosteoporotic agent for bone and calcium metabolic dysfunctions [35]. It has been used as an oral gastrointestinal contrast agent, achieving high-contrast imaging of the mouse gastrointestinal tract during CT examinations, and it is not accompanied by adverse reactions such as physical discomfort or acute poisoning [36,31].

Previous studies have shown that liquid metal gallium can flow into the nano-scale microvascular network in vitro in organs such as the heart and kidney, and its fluidity is far better than that of traditional iodinated contrast agents. It does not damage the corresponding tissue structures [37]. In this study, we reported the value of liquid metal gallium for use as an angiographic contrast agent in CT angiography of the liver in vivo. Hepatic artery angiography and abdominal enhanced CT scans of New Zealand white rabbits were performed by femoral artery puncture [38] using liquid metal gallium with a purity of 99.99% compared with ioversol. The results including the artery imaging effect, overall image quality, and the incidence of adverse events were compared between the two contrast agent groups. The overall imaging effect and the in vivo biological safety of liquid metal gallium in CT hepatic angiography were evaluated.

Materials And Methods

Contrast agents

A total of two contrast agents were used in this study. The experimental group had liquid metal gallium applied as a vascular contrast agent with a purity of >99.99% provided by the Technical Institute of Physics and Chemistry of the Chinese Academy of Sciences; the control group had ioversol contrast agent applied (Optiray, 320 mg/mL) from the Vanlink Corporation.

Experimental animals

This experiment was approved by the hospital ethics committee and complied with the “Regulations on Laboratory Animal Management” published by the Chinese government. The Institute of Experimental Animals of the General Hospital of the People’s Liberation Army provided 30 female New Zealand white rabbits for experimental use, weighing approximately 3.5-4 kg, and aged 5-6 months. They fasted for 24 hours before the experiment and were weighed before the procedure.

Experiment equipment

A 64-row Siemens SOMATOM Definition Flash CT scanner; Double-syringe power injector (Stellant D, USA); CT image post-processing workstation (GE AW4.6); 3F intervention microcatheter (Terumo, Japan); ophthalmic tweezers and ophthalmic scissors; and an anti-blood reflux valve were used during the procedure.

Hepatic angiography

Thirty rabbits were randomly divided into the experimental group and control group, with 15 rabbits in each, and they were given numbers. After weighing, each rabbit was anaesthetized and the rabbit’s abdomen was fixed on the CT scanning bed with an abdominal band. The skin and fascia were cut

longitudinally in the pulsating area of the rabbit's right inguinal region after skin preparation, sterilization, and draping. The length of the incision was 3.0~4.0 cm. Then, the muscle and femoral artery sheath were bluntly separated, and approximately 2.0 cm of the femoral artery was exposed. Under the guidance of the CT scan, the tip of the 3F microcatheter was quickly placed in the opening of the celiac trunk about the twelfth thoracic vertebrae level through the femoral artery puncture method (Fig. 2a), and the wire guide was removed and 0.5 ml of 1% lidocaine was injected through the catheter.

The control group was given ioversol contrast agent, and the experimental group was given liquid metal gallium as the vascular contrast agent (purity > 99.99%). The contrast agent and the saline solution were drawn into a double-syringe power injector, and then we connected the infusion tube to the detained trocar of the rabbit femoral artery. The experimental group and the control group were successively injected with 6~7.5 ml of contrast agent and normal saline through the femoral artery after a plain CT scan of the abdomen, and we then performed hepatic angiography and abdominal CT with contrast enhancement. The injection rate was 1.5 ml/s, and the injection time was 4 seconds in both the experimental group and the control group, except for the rabbits with a large liver parenchyma during the plain CT scan who were injected for 5 seconds. After the experiment, the contrast catheter was pulled out, the surgical incision was sutured, and 800,000 U of penicillin was continuously injected intramuscularly for 3 days after the operation.

CT inspection method and image post-processing

The dynamic spiral CT scan range is from approximately 3 cm above the top of the diaphragm to the bifurcation of the arteria iliaca communis. The machine speed is 0.28 s/360°, the tube voltage is 100 kV, the tube current is 100 mA, the layer thickness and the layer spacing are both 3 mm, and the thread pitch is 0.984:1. The reconstruction layer thickness and layer spacing are both 1 mm. Finally, all of the obtained data were transmitted to a GE AW4.6 workstation for data post-processing. CT image post-processing technologies included multiplanar reformation (MPR), maximum intensity projection (MIP) and volume rendering (VR).

Measurement and calculation of the CT data

After anonymizing them as to which contrast agent was used, the two groups of CT images were independently post-processed by two physicians who have been engaged in abdominal imaging diagnosis for more than 5 years, and regions of interest (ROI) were delineated, measured and calculated, including: 1) Three-dimensional vascular reconstruction of the abdominal aorta and hepatic artery, along with the measurement of the smallest hepatic artery diameter (mm) on the CT axial images. 2) Measurement of the CT values of the liver parenchyma and abdominal aorta in the plain and arterial phases and the standard deviation (SD) of the corresponding liver parenchyma at a level about 3 mm above or below the bifurcation of the celiac trunk. 3) Measurement of the CT value of the hepatic artery in the arterial phase. The area of interest (ROI) of the liver parenchyma was selected from the non-vascular

and bile duct areas of the left lateral lobe approximately 3 mm from the edge, the size of the ROI was nearly 20 mm² (Fig. 2b), the size of the abdominal aorta ROI was approximately 10 mm² (Fig. 2b), and the hepatic artery ROI was selected for the arterial imaging area of the left lobe about 3 mm from the edge of the liver, and its size was approximately 1.5 mm² (Fig. 2c). The size, shape, and height of the ROI for each part was required to be consistent across the images. Then, we took the average of the data measured by the two physicians on the same experimental rabbit, including: Absolute enhancement CT value of the liver parenchyma and abdominal aorta: absolute enhancement CT value (HU)= CT value after enhancement-CT value during the plain scan. CT difference between the hepatic artery and liver parenchyma in the arterial phase; CT difference between the abdominal aorta and the liver parenchyma in the arterial phase. Contrast-to-noise ratio (CNR) of the hepatic artery and abdominal aorta in the arterial phase, CNR=(CT (target vessel)-CT (same layer of the liver parenchyma))/SD (same layer of the liver parenchyma) [39].

Image quality assessments

Two doctors who have been engaged in imaging diagnosis for more than 5 years independently assessed the image quality of the two groups. The evaluation criteria were: Superior, the image showed that the abdominal aorta and hepatic artery were completely filled with contrast agent, and the subtle structure of the blood vessels and surrounding tissues could be clearly seen; Medium, the image showed that the abdominal aorta and hepatic artery had a relatively good filling effect, but the tiny structure of the arteries' surrounding tissues was not well displayed; Inferior, the image displayed that the filling effect of the abdominal aorta and hepatic artery was poor, and the microstructure of the surrounding tissues was poorly visible. We calculated the excellent and good rates of the two groups in terms of image quality, where the excellent and good rate = (number of superior cases + number of medium cases)/total number of cases * 100%. When the two doctors disagreed on the quality evaluation of the same image, a third doctor with more seniority re-evaluated the image and we applied the same evaluation index.

Follow-up

This study closely observed and recorded the diet, defecation, and activity status of each rabbit within 3 days after the angiography examination, as well as the presence or absence of contrast agent retention on the abdominal CT plain scan conducted 24 hours after the angiography examination.

Statistical analysis

The measurement data from the two groups are expressed as the mean ± standard deviation (SD), and the enumeration data are expressed as the number of cases (n) and percentage (%). Statistical analysis was performed using SPSS 24.0 statistical analysis software. The independent sample t-test was used to

compare the sample means of the two groups. P < 0.05 means that the difference is statistically significant.

Results And Discussion

Contrast CT imaging of arteries and liver parenchyma

All catheter tips were successfully placed at the bifurcation of the abdominal aorta near the coeliac trunk. In addition, there was no problem with the CT angiography of ioversol or the liquid metal gallium. The experimental group and the control group showed significant differences in the enhancement of the hepatic artery, abdominal aorta and liver parenchyma (P <0.001) (Table.1). The absolute enhanced CT value of the liver parenchyma of the control group was significantly higher than that of the experimental group, as shown in Table 1 and Figure 3. The absolute enhancement CT value of the abdominal aorta of the experimental group was significantly higher than that of the control group, as shown in Table 1 and Figure 4a. The average CT value of the hepatic artery in the arterial phase between the control group and the experimental group was significantly different (Table 1 and Fig. 4b).The smallest vascular diameter of the hepatic artery in the control group was significantly larger than that in the experimental group, as shown in Table 1 and Figure 5. The CNR of the hepatic artery and the CNR of the abdominal aorta in the arterial phase of the control group were significantly lower than those of the experimental group, as shown in Table 1 and Figure 6.

Table 1
Summary of CT imaging data

	Mean (± SD)		T	P
	Control group	Experimental group		
Average CT value of liver parenchyma HU	144.97 (3.54)	79.8 (4.14)	49.28	<0.001
Mean CT value of abdominal aorta HU	220.21 (6.05)	2277.17 (417.98)	-19.12	<0.001
Average CT value of hepatic artery HU	225.44 (7.58)	542.61 (38.35)	-29.93	<0.001
Minimum vessel diameter of hepatic artery mm	1.3 (0.09)	0.83 (0.06)	17.94	<0.001
$CT_{hepatic\ artery}$-$CT_{liver\ parenchyma}$ HU	80.47 (8.45)	462.81 (38.27)	-35.49	<0.001
$CT_{abdominal\ aorta}$ – $CT_{liver\ parenchyma}$ HU	75.24 (3.76)	2197.37 (416.61)	-19.79	<0.001
$CT_{liver\ parenchyma\ in\ arterial\ phase}$ -$CT_{liver\ parenchyma\ during\ plain\ scan}$ HU	86.5 (4.85)	21.33 (4.78)	49.28	<0.001
$CT_{abdominal\ aorta\ in\ arterial\ phase}$ -$CT_{abdominal\ aorta\ during\ plain\ scan}$ HU	173.78 (6.76)	2230.74 (417.7)	-19.12	<0.001
CNR of hepatic artery during enhancement phase	16.48 (2.9)	59.03 (10.07)	-15.2	<0.001
CNR of abdominal aorta during enhancement phase	15.41 (2.31)	277.28 (53.51)	-19.5	<0.001

CT image quality

The overall CT image quality of the two contrast examinations are shown in Table 2 and Fig 7. The excellent and good rate of CT image quality in the ioversol group was significantly higher than that of the liquid metal gallium group, and the difference was statistically significant ($P < 0.05$). The two types of CT images showed that liquid metal gallium angiography had a better vascular enhancement effects in the hepatic artery and abdominal aorta than ioversol, and liquid metal gallium angiography was superior to ioversol for viewing the microvascular ends (Fig 8, 9). However, the liquid metal gallium angiography has a high X-ray attenuation coefficient, so the enhanced CT images of experimental group contains metal artefacts, which reduces the overall image quality(Fig 2c).

Table 2
Summary of image quality data

	Number of cases (n)	Superior (n)	Medium (n)	Inferior (n)	Excellent and good rate (%)
Control group	15	8	5	2	86.67%*
Experimental group	15	0	8	7	53.33%*
*p < 0.05					

Postoperative observations

The experimental group had various adverse events such as inappetence, abnormal defecation and urination, decreased mobility, and slow contrast media metabolism within 3 days after the examination. The incidence of adverse events in the experimental group was significantly higher than that of the control group, and the difference was statistically significant (P < 0.001), shown in Table 3.

Table 3
Summary of adverse events data

	Number of cases n	Inappetence (%)	Abnormal defecation and urination n (%)	Decreased mobility n (%)	Contrast agent retention after 24 hours n (%)	Adverse event rate (%)
Control group	15	5(33.33%)	2(13.33%)	6(40%)	3(20%)	26.67%*
Experimental group	15	9(60%)	8(53.33%)	11(73.33%)	15(100%)	100%*
*p < 0.05						

CT angiography (CTA) technology is an important method for clinical understanding of the vascular anatomy, clarifying the location of vascular lesions, judging the blood supply to parenchymal lesions, and selecting appropriate therapeutic schemes. CTA technology is also the key to improving the level of clinical diagnosis and treatment, realizing the visualization of the in vivo vascular system, and reducing mortality from cardiovascular and cerebrovascular diseases [40,41]. Contrast agent plays an important role in CTA imaging [42]. Therefore, in order to better display the complex microcapillary network system in living tissues, special attention needs to be paid to the selection of contrast agents. At present, in order to increase the contrast between the blood vessels and the surrounding parenchyma, researchers mostly

start by adjusting the solute density in the contrast agent solution. Therefore, a variety of metal materials such as lead and bismuth have been studied as vascular contrast agents, but they have inevitable limitations such as high melting points, volume shrinkage during the hardening processes and difficult discharge from the body [43,44].

The results of this study showed that the CT enhancement effect of liquid gallium used as an angiographic contrast agent can show a finer biological vascular distribution system than ioversol, and it has high contrast between vessels and surrounding tissues, which is suitable for three-dimensional vascular reconstruction technology in CT examinations. The use of liquid metal gallium as an angiographic contrast agent is expected to open up a new approach to microvascular imaging that is different from traditional capillary imaging.

In this study, the average diameter of the smallest hepatic artery shown by liquid metal gallium was approximately 0.6 mm, which failed to reach the micron level shown in the study of isolated kidneys [37]. We consider the reason for this is that liquid metal gallium has blood dilution in living blood transport, and it has a problem of contrast agent diffusion under the action of the osmotic pressure of living vessels. The results of this study showed that liquid metal gallium has large metal hard ray artefacts on CTA and it has an insignificant enhancement effect on perivascular tissues, which introduces certain difficulties into clinical diagnosis. Therefore, it is necessary to correct for the metal artefacts in the reconstructed CT images.

Metal artefact correction algorithms are mainly divided into three categories: iterative reconstruction algorithms [45], projection interpolation algorithms [46], and a combination of iteration and interpolation [47]. The iterative algorithm performs iterative reconstruction of the projection data of metal objects according to certain criteria. Compared with the projection interpolation algorithm, it can effectively remove the metal artefacts and correct the image to yield a higher quality [48]. In addition, this study showed that liquid metal gallium is discharged slowly from the body, which seriously affects the body's activity, food consumption, and defecation, and its biological safety is low. Therefore, the use of liquid metal gallium as a contrast agent for CT angiography still needs additional molecular biology research to develop its molecular structure in the direction of higher vascular permeability.

Summary And Conclusions

In this paper, we introduced liquid metal gallium can show subtle vascular structure and high contrast between vessels and the surrounding tissues in CT angiography of living organs that is better than that seen with traditional iodinated contrast agents. Our study is the first to explore the application value of liquid metal gallium in CT angiography of living organs.What’s more, the results demonstrated that liquid metal gallium used as a CT angiography contrast agent has large metal artefacts and low biological safety. It needs to be combined with nano-microsphere packaging technology [49], metal artefact correction algorithms and water-soluble molecular structure improvement technology and other related materials research before considering its use in the clinic.

Declarations

Acknowledgements

The authors would like to thank Chen Peng of Third Medical Centre of Chinese PLA General Hospital for technical assistance in animal experiments. The authors also acknowledge the financial support from the National Key R&D Program of China (Contact Grant Number: 2019YFC0118104) and the Capital characteristic clinical research of China (Contact Grant Number:Z101100001718013).

Author contributions

T.Liu and G.S.Wang proposed the problem and was responsible of the discussion and writing of the manuscript. J.W.Zhao and T.Liu prepared material and conducted the experiments. H.Liu and W.J.Han analyzed the results and prepared figures. Z.Y.Zhang and X.X.Chen revised and approved the final manuscript.

Additional Information

All authors can prove that we have full control of all primary data and we agree to allow the journal to review our data if requested. What's more, we are declare that we have no conflict of interest.

Compliance with ethical standards

References

1. Wickström, J. E., Jalkanen, J. M., Venermo, M. & Hakovirta, H. H. Crural Index and extensive atherosclerosis of crural vessels are associated with long-term cardiovascular mortality in patients with symptomatic peripheral artery disease. *Atherosclerosis* **264**, 44-50. https://doi.org/10.1016/j.atherosclerosis.2017.07.023 (2017).
2. Hounsfield, G. N. Computerized transverse axial scanning (tomography): Part I. Description of system. 1973. *Br J Radiol* **68**, H166-172 (1995).
3. Dewey, M. *et al.* Noninvasive coronary angiography by 320-row computed tomography with lower radiation exposure and maintained diagnostic accuracy: comparison of results with cardiac catheterization in a head-to-head pilot investigation. *Circulation* **120**, 867-875. https://doi.org/10.1161/CIRCULATIONAHA.109.859280 (2009).
4. Shah, N. R., Blankstein, R., Villines, T., Imran, H., Morrison, A. R. & Cheezum, M. K. Coronary CTA for Surveillance of Cardiac Allograft Vasculopathy. *Curr Cardiovasc Imaging Rep* **11**, 26. https://doi.org/10.1007/s12410-018-9467-z. Epub 2018 Sep 24 (2018).
5. Montet, X., Pastor, C. M., Vallée, J. P., Becker, C. D., Geissbuhler, A., Morel, D. R. & Meda, P. Improved visualization of vessels and hepatic tumors by micro-computed tomography (CT) using iodinated

liposomes. *Invest Radiol* **42**, 652-658. https://doi.org/10.1097/RLI.0b013e31805f445b (2007).

6. Imai, K., Ikeda, M., Satoh, Y., Fujii, K., Kawaura, C., Nishimoto, T. & Mori, M. Contrast enhancement efficacy of iodinated contrast media: Effect of molecular structure on contrast enhancement. *Eur J Radiol Open* **5**, 183-188. https://doi.org/10.1016/j.ejro.2018.09.005 (2018).
7. Hallouard, F., Anton, N., Choquet, P., Constantinesco, A. & Vandamme, T. Iodinated blood pool contrast media for preclinical X-ray imaging applications--a review. *Biomaterials* **31**, 6249-6268. https://doi.org/10.1016/j.biomaterials.2010.04.066 (2010).
8. Mortelé, K. J., Oliva, M. R., Ondategui, S., Ros, P. R. & Silverman, S. G. Universal use of nonionic iodinated contrast medium for CT: evaluation of safety in a large urban teaching hospital. *AJR Am J Roentgenol* **184**, 31-34. https://doi.org/10.2214/ajr.184.1.01840031 (2005).
9. Ogawa, M., Kawaguchi, Y., Kawashima, Y., Mizukami, H., Maruno, A., Ito, H. & Mine, T. Comparison of ionic, monomer, high osmolar contrast media with non-ionic, dimer, iso-osmolar contrast media in ERCP. *Tokai J Exp Clin Med* **38**, 109-113 (2013).
10. Andreucci, M., Solomon, R. & Tasanarong, A. Side effects of radiographic contrast media: pathogenesis, risk factors, and prevention. *Biomed Res Int* **2014**, 741018. https://doi.org/10.1155/2014/741018 (2014).
11. Seong, J. M. *et al.* Comparison of the safety of seven iodinated contrast media. *J Korean Med Sci* **28**, 1703-1710. https://doi.org/10.3346/jkms.2013.28.12.1703 (2013).
12. Meurer, K., Laniado, M., Hosten, N., Kelsch, B. & Hogstrom, B. Intra-arterial and intravenous applications of Iosimenol 340 injection, a new non-ionic, dimeric, iso-osmolar radiographic contrast medium: phase 2 experience. *Acta Radiol* **56**, 702-708. https://doi.org/10.1177/0284185114536157 (2015).
13. Palkowitsch, P. K., Bostelmann, S. & Lengsfeld, P. Safety and tolerability of iopromide intravascular use: a pooled analysis of three non-interventional studies in 132,012 patients. *Acta Radiol* **55**, 707-714. https://doi.org/10.1177/0284185113504753 (2014).
14. Meth, M. J. & Maibach, H. I. Current understanding of contrast media reactions and implications for clinical management. *Drug Saf* **29**, 133-141. https://doi.org/10.2165/00002018-200629020-00003 (2006).
15. Callahan, M. J., Poznauskis, L., Zurakowski, D. & Taylor, G. A. Nonionic iodinated intravenous contrast material-related reactions: incidence in large urban children's hospital--retrospective analysis of data in 12,494 patients. *Radiology* **250**, 674-681. https://doi.org/10.1148/radiol.2503071577 (2009).
16. Cha, M. J. *et al.* Hypersensitivity Reactions to Iodinated Contrast Media: A Multicenter Study of 196 081 Patients. *Radiology* **293**, 117-124. https://doi.org/10.1148/radiol.2019190485 (2019).
17. Hossain, M. A. *et al.* Contrast-induced nephropathy: Pathophysiology, risk factors, and prevention. *Saudi J Kidney Dis Transpl* **29**, 1-9. https://doi.org/10.4103/1319-2442.225199 (2018).
18. Krasinski, Z., Krasińska, B., Olszewska, M. & Pawlaczyk, K. Acute Renal Failure/Acute Kidney Injury (AKI) Associated with Endovascular Procedures. *Diagnostics (Basel)* **10**,

https://doi.org/10.3390/diagnostics10050274 (2020).

19. Faucon, A. L., Bobrie, G. & Clément, O. Nephrotoxicity of iodinated contrast media: From pathophysiology to prevention strategies. *Eur J Radiol* **116**, 231-241. https://doi.org/10.1016/j.ejrad.2019.03.008 (2019).
20. Burchardt, P. *et al.* Early renal dysfunction after contrast media administration despite prophylactic hydration. *Int J Cardiovasc Imaging* **29**, 959-966. https://doi.org/10.1007/s10554-013-0186-x (2013).
21. Einhorn, L. Gallium nitrate in the treatment of bladder cancer. *Semin Oncol* **30**, 34-41. https://doi.org/10.1016/s0093-7754(03)00174-x (2003).
22. Sun, X., He, Z. Z., Deng, Z. S., Zhou, Y. X. & Liu, J. Liquid metal bath as conformable soft electrodes for target tissue ablation in radio-frequency ablation therapy. *Minim Invasive Ther Allied Technol* **27**, 233-241. https://doi.org/10.1080/13645706.2017.1393437 (2018).
23. Krishnamurthi, V. *et al.* Liquid-Metal Synthesized Ultrathin SnS Layers for High-Performance Broadband Photodetectors. *Adv Mater* **32**, e2004247. https://doi.org/10.1002/adma.202004247 (2020).
24. Foster, B. J., Clagett-Carr, K., Hoth, D. & Leyland-Jones, B. Gallium nitrate: the second metal with clinical activity. *Cancer Treat Rep* **70**, 1311-1319 (1986).
25. Collery, P., Keppler, B., Madoulet, C. & Desoize, B. Gallium in cancer treatment. *Crit Rev Oncol Hematol* **42**, 283-296. https://doi.org/10.1016/s1040-8428(01)00225-6 (2002).
26. Warrell, R. P. Jr, Coonley, C. J., Straus, D. J. & Young, C. W. Treatment of patients with advanced malignant lymphoma using gallium nitrate administered as a seven-day continuous infusion. *Cancer* **51**, 1982-1987. https://doi.org/10.1002/1097-0142(19830601)51:11<1982::aid-cncr2820511104>3.0.co;2-l (1983).
27. Straus, D. J. Gallium nitrate in the treatment of lymphoma. *Semin Oncol* **30**, 25-33. https://doi.org/10.1016/s0093-7754(03)00173-8 (2003).
28. Casper, E. S., Stanton, G. F., Sordillo, P. P., Parente, R., Michaelson, R. A. & Vinceguerra, V. Phase II trial of gallium nitrate in patients with advanced malignant melanoma. *Cancer Treat Rep* **69**, 1019-1020 (1985).
29. Malfetano, J. H., Blessing, J. A. & Adelson, M. D. A phase II trial of gallium nitrate (NSC #15200) in previously treated ovarian carcinoma. A Gynecologic Oncology Group Study. *Am J Clin Oncol* **14**, 349-351. https://doi.org/10.1097/00000421-199108000-00015 (1991).
30. Chitambar, C. R. Gallium compounds as antineoplastic agents. *Curr Opin Oncol* **16**, 547-552. https://doi.org/10.1097/01.cco.0000142071.22226.d2 (2004).
31. Chitambar, C. R. Medical applications and toxicities of gallium compounds. *Int J Environ Res Public Health* **7**, 2337-2361. https://doi.org/10.3390/ijerph7052337 (2010).
32. Olakanmi, O., Gunn, J. S., Su, S., Soni, S., Hassett, D. J. & Britigan, B. E. Gallium disrupts iron uptake by intracellular and extracellular Francisella strains and exhibits therapeutic efficacy in a murine pulmonary infection model. *Antimicrob Agents Chemother* **54**, 244-253. https://doi.org/10.1128/AAC.00655-09 (2010).

33. Thompson, M. G. *et al.* Evaluation of Gallium Citrate Formulations against a Multidrug-Resistant Strain of Klebsiella pneumoniae in a Murine Wound Model of Infection. *Antimicrob Agents Chemother* **59**, 6484-6493. https://doi.org/10.1128/AAC.00882-15 (2015).
34. Goss, C. H. *et al.* Gallium disrupts bacterial iron metabolism and has therapeutic effects in mice and humans with lung infections. *Sci Transl Med* **10**, https://doi.org/10.1126/scitranslmed.aat7520 (2018).
35. Verron, E., Bouler, J. M. & Scimeca, J. C. Gallium as a potential candidate for treatment of osteoporosis. *Drug Discov Today* **17**, 1127-1132. https://doi.org/10.1016/j.drudis.2012.06.007 (2012).
36. Liu, H., Yu, Y., Wang, W., Liu, Y., An, Y., Wang, Q. & Liu, J. Novel contrast media based on the liquid metal gallium for in vivo digestive tract radiography: a feasibility study. *Biometals* **32**, 795-801. https://doi.org/10.1007/s10534-019-00212-5 (2019).
37. Wang, Q., Yu, Y., Pan, K. & Liu, J. Liquid metal angiography for mega contrast X-ray visualization of vascular network in reconstructing in-vitro organ anatomy. *IEEE Trans Biomed Eng* **61**, 2161-2166. https://doi.org/10.1109/TBME.2014.2317554 (2014).
38. Feldman, D. N. *et al.* Adoption of radial access and comparison of outcomes to femoral access in percutaneous coronary intervention: an updated report from the national cardiovascular data registry (2007-2012). *Circulation* **127**, 2295-2306. https://doi.org/10.1161/CIRCULATIONAHA.112.000536 (2013).
39. Lenfant, M. *et al.* Deep Learning Versus Iterative Reconstruction for CT Pulmonary Angiography in the Emergency Setting: Improved Image Quality and Reduced Radiation Dose. *Diagnostics (Basel)* **10**, https://doi.org/10.3390/diagnostics10080558 (2020).
40. Forsting, M. CTA of the ICA bifurcation and intracranial vessels. *Eur Radiol* **15 Suppl 4**, D25-27. https://doi.org/10.1007/s10406-005-0120-y (2005).
41. Leithner, D., Wichmann, J. L., Mahmoudi, S., Martin, S. S., Albrecht, M. H., Vogl, T. J. & Scholtz, J. E. Diagnostic yield of 90-kVp low-tube-voltage carotid and intracerebral CT-angiography: effects on radiation dose, image quality and diagnostic performance for the detection of carotid stenosis. *Br J Radiol* **91**, 20170927. https://doi.org/10.1259/bjr.20170927 (2018).
42. Guerrisi, A. *et al.* Effect of varying contrast material iodine concentration and injection technique on the conspicuity of hepatocellular carcinoma during 64-section MDCT of patients with cirrhosis. *Br J Radiol* **84**, 698-708. https://doi.org/10.1259/bjr/21539234 (2011).
43. Frezza, M., Hindo, S., Chen, D., Davenport, A., Schmitt, S., Tomco, D. & Dou, Q. P. Novel metals and metal complexes as platforms for cancer therapy. *Curr Pharm Des* **16**, 1813-1825. https://doi.org/10.2174/138161210791209009 (2010).
44. Jakupec, M. A. & Keppler, B. K. Gallium and other main group metal compounds as antitumor agents. *Met Ions Biol Syst* **42**, 425-462 (2004).
45. Schabel, C. *et al.* Improving CT-Based PET Attenuation Correction in the Vicinity of Metal Implants by an Iterative Metal Artifact Reduction Algorithm of CT Data and Its Comparison to Dual-Energy-Based

Strategies: A Phantom Study. *Invest Radiol* **52**, 61-65. https://doi.org/10.1097/RLI.0000000000000306 (2017).

46. Veldkamp, W. J., Joemai, R. M., van der Molen, A. J. & Geleijns, J. Development and validation of segmentation and interpolation techniques in sinograms for metal artifact suppression in CT. *Med Phys* **37**, 620-628. https://doi.org/10.1118/1.3276777 (2010).
47. Watzke, O. & Kalender, W. A. A pragmatic approach to metal artifact reduction in CT: merging of metal artifact reduced images. *Eur Radiol* **14**, 849-856. https://doi.org/10.1007/s00330-004-2263-y (2004).
48. André, F. *et al.* Improved image quality with simultaneously reduced radiation exposure: Knowledge-based iterative model reconstruction algorithms for coronary CT angiography in a clinical setting. *J Cardiovasc Comput Tomogr* **11**, 213-220. https://doi.org/10.1016/j.jcct.2017.02.007 (2017).
49. Nel, A. E. *et al.* Understanding biophysicochemical interactions at the nano-bio interface. *Nat Mater* **8**, 543-557. https://doi.org/10.1038/nmat2442 (2009).

Figures

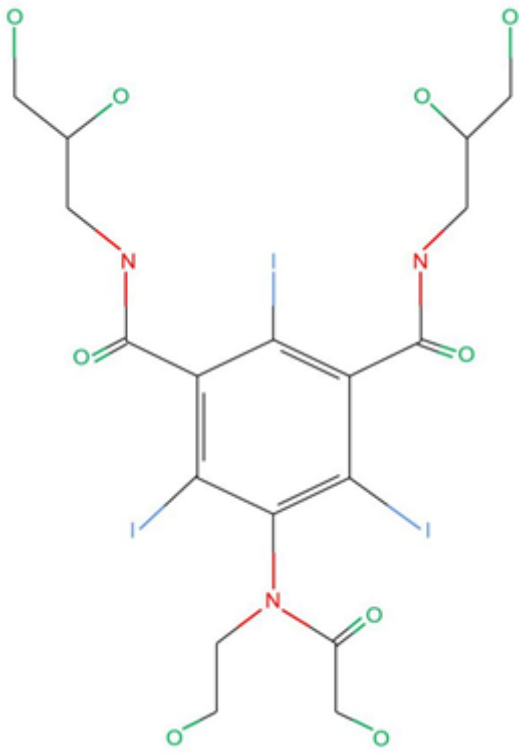

Figure 1

Molecular structure of the non-ionic monomeric contrast agent of ioversol

Figure 2

Representative CT images from the Control and Experimental group a The tip of the 3F microcatheter was placed at the level of the abdominal aorta about the 12th thoracic vertebra under the CT-guided transfemoral puncture.b and c The size of the regions of interest (ROI) of the liver parenchyma(b), abdominal aorta (b) and hepatic artery(c) was 19.4 mm2, 10.9 mm2, and 1.4 mm2 respectively

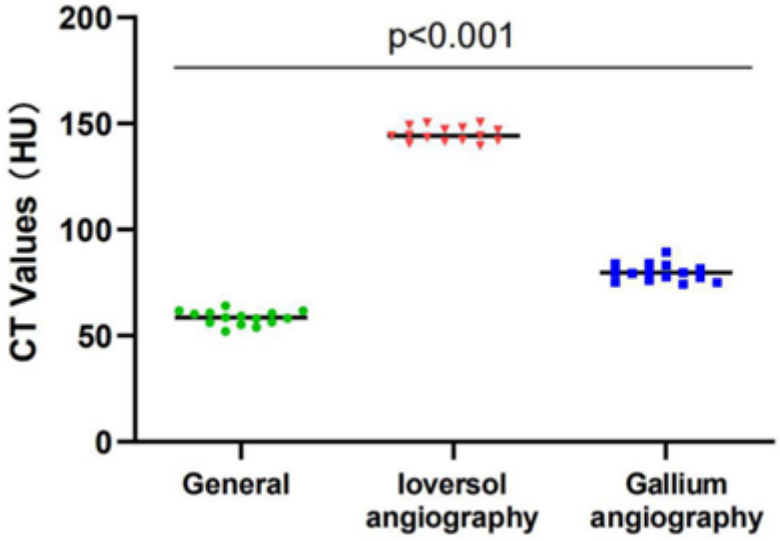

Figure 3

The average CT value of the liver parenchyma of the Plian scan, Control group and Experimental group

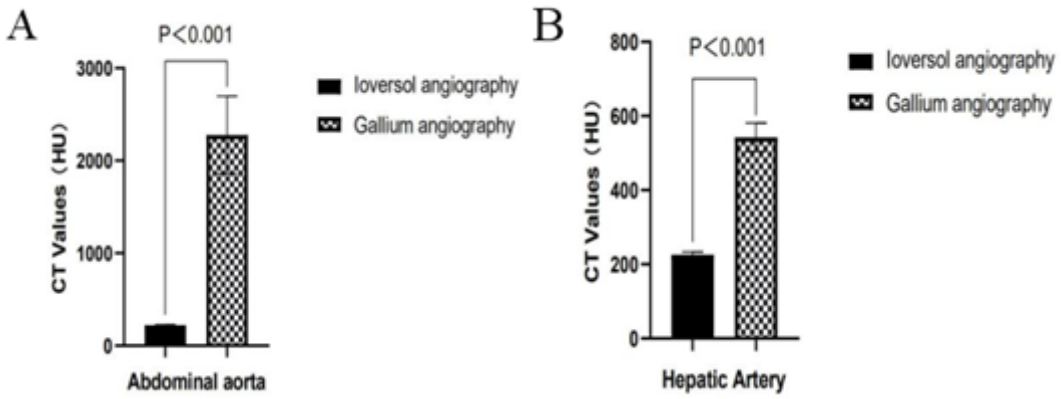

Figure 4

Mean values of the enhanced CT scan of the abdominal aorta and hepatic artery a The absolute enhancement CT value of the abdominal aorta of the experimental group was significantly higher than that of the control group.b The average CT value of the hepatic artery in the arterial phase between the control group and the experimental group was significantly different.

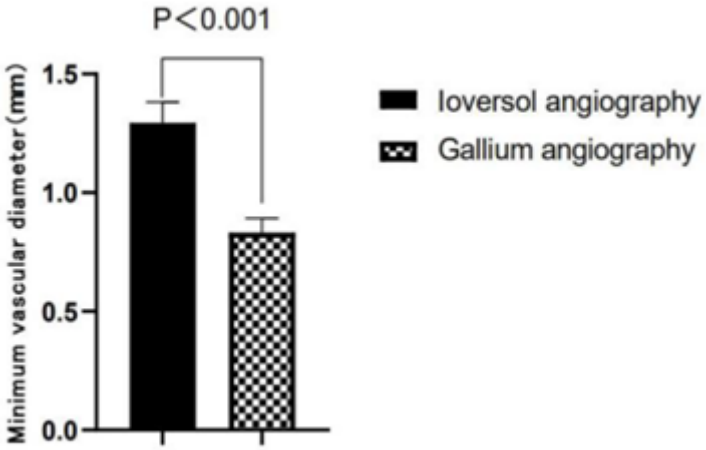

Figure 5

The smallest hepatic artery diameter of the Control group and Experimental group

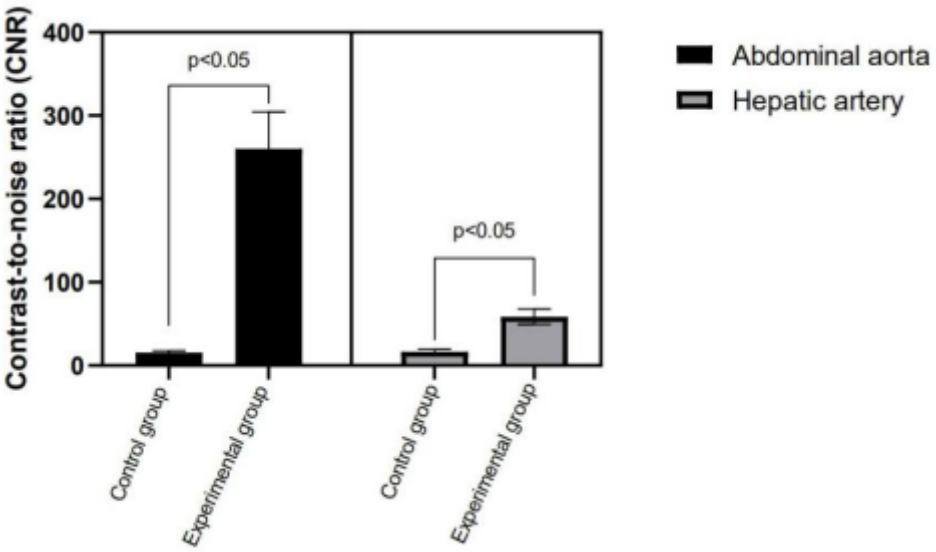

Figure 6

The contrast-to-noise ratio (CNR) of the abdominal aorta and hepatic artery in the Control group and Experimental group

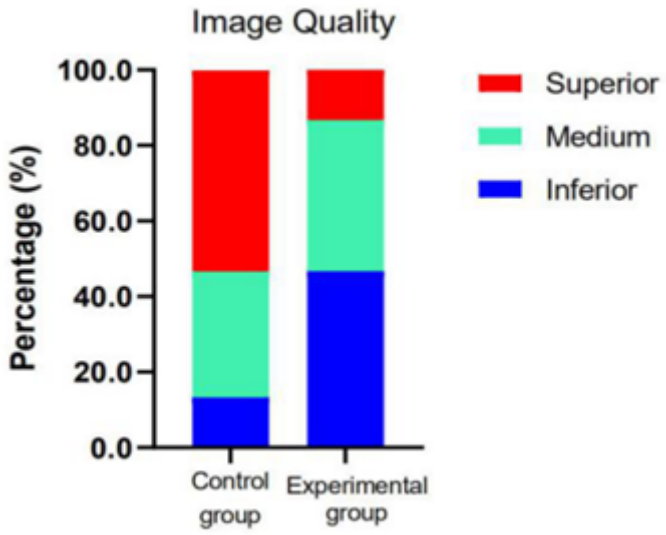

Figure 7

Image quality of the abdominal enhanced CT examination The excellent and good rate of CT image quality in the ioversol group was significantly higher than that of the liquid metal gallium group

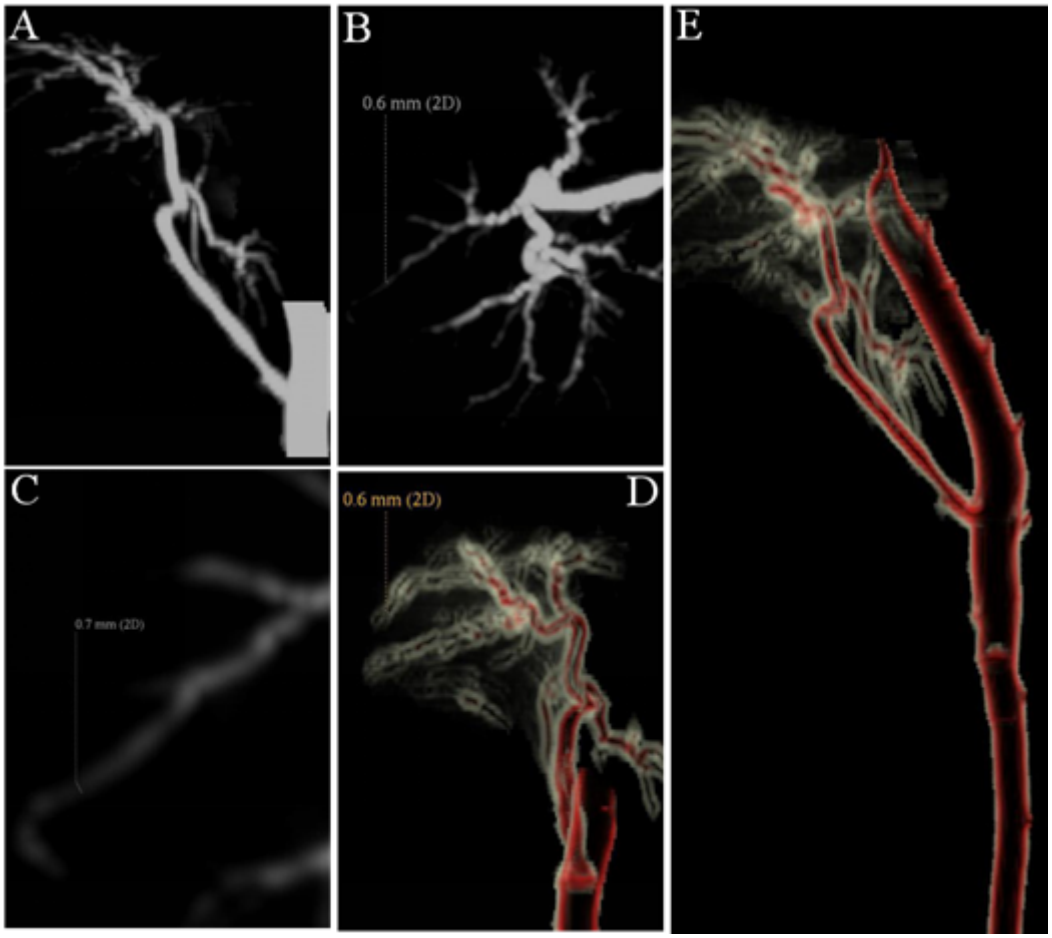

Figure 8

CT images of liquid metal gallium CT angiography MIP imaging (a, b, c) and MPR imaging (d,e) of abdominal aorta and hepatic artery shows the microvascular end's diameter is 0.6mm.

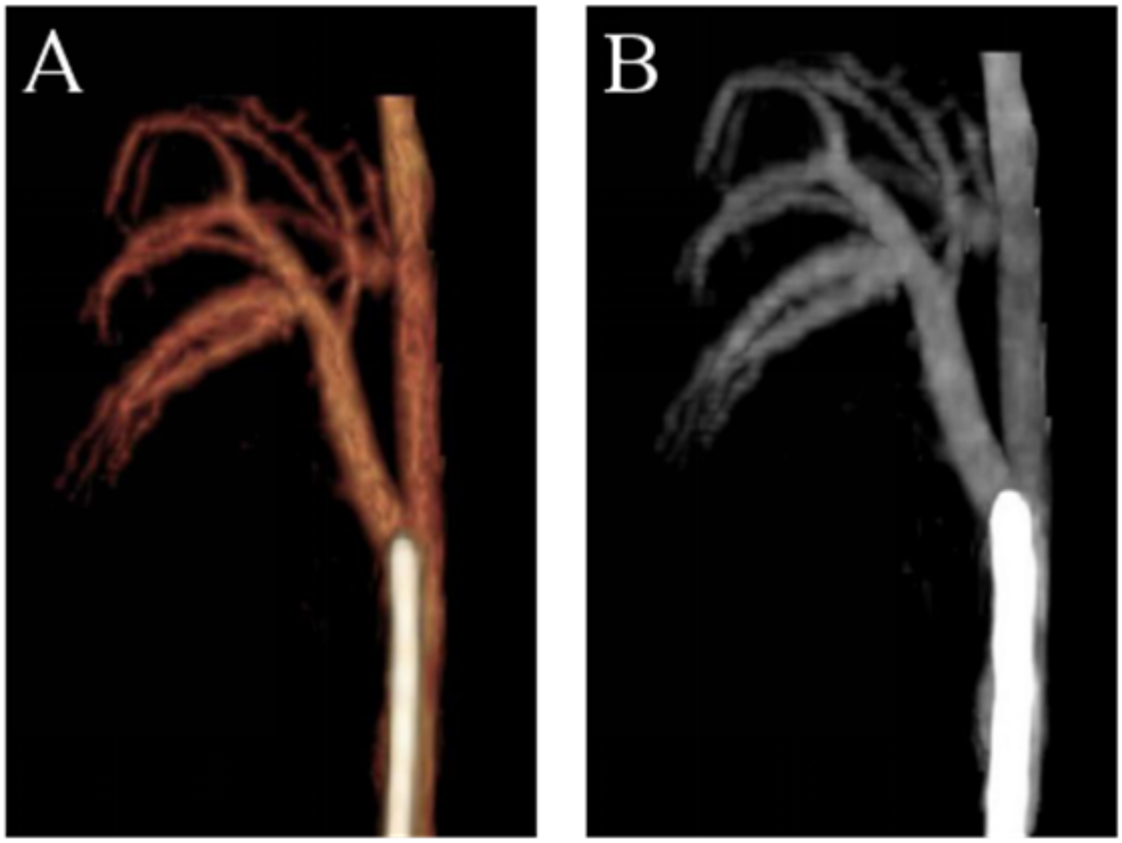

Figure 9

CT images of Ioversol CT angiography VR imaging (a) and MIP imaging (b) of abdominal aorta and hepatic artery